

Techno-economic analysis of geothermal desalination using Hot Sedimentary Aquifers: A pre-feasibility study for Western Australia

Alexander Christ ^{b,c}, Bijan Rahimi ^{b,d}, Klaus Regenauer-Lieb ^e, Hui Tong Chua ^{a,b,*}

^a College of Environmental Science and Engineering, Taiyuan University of Technology, Taiyuan 030024, China

^b School of Mechanical and Chemical Engineering, The University of Western Australia, 35 Stirling Hwy, Perth, WA 6009, Australia

^c School of Earth and Environment, The University of Western Australia, 35 Stirling Hwy, Crawley, WA 6009, Australia

^d Institute of Water and Energy (IWE), Sharif University of Technology, Azadi Ave., Tehran, Iran

^e School of Petroleum Engineering, The University of New South Wales, 330 Anzac Parade, Kensington, NSW 2033, Australia



HIGHLIGHTS

- A validated techno-economic model for geothermal desalination has been developed.
- The model incorporates a validated hydrodynamic pumping model for the geothermal fluid.
- The Preheated Boosted MED technology has been considered.
- The economic viability of geothermal desalination in Western Australia has been demonstrated.

ARTICLE INFO

Article history:

Received 9 May 2016

Received in revised form 26 October 2016

Accepted 6 November 2016

Available online 17 November 2016

Keywords:

Geothermal

Desalination

Cost

MED

Pumping power

Aquifer

ABSTRACT

This work offers an extensive framework for the techno-economic evaluation of the subsurface and surface components of low-grade geothermal (<100 °C) desalination systems, that is based on validated hydrogeological, thermodynamic, and economic considerations. Additionally, this work incorporates a recently developed advanced multi-effect distillation (MED) process for an improved utilisation of the geothermal heat sources. The analysis focuses on a pre-feasibility study for Western Australia, the influence of the different cost drivers, especially the often overlooked geothermal well field parameters like permeability, so as to permit rational assessments of potential application sites. For the surveyed area in Western Australia, the confluence of geothermal and desalination systems results in a promising and economically viable alternative water source.

© 2016 Elsevier B.V. All rights reserved.

1. Introduction

Geothermal energy is a promising renewable energy. Its climatic, diurnal and seasonal independent characteristic allows for a quantifiable, reliable and extremely stable energy supply, which is perfect for desalination.

In 1959 Bell [1] conducted an economic analysis of a 75 m³/day geothermal driven Multi-Effect-Evaporation plant. A decade later, the US Department of Reclamation in California attempted to generate freshwater directly from high temperature (>150 °C) geothermal fluid [2]. Different desalination methods have since been evaluated [3,4], including a Multi Stage Flash (MSF) and a Vertical-Tube-Evaporator (VTE) pilot plant [5]. The first patent of a desalination unit designed for high-enthalpy geothermal sites was issued in 1976 [6]. In 1982, Ophir

[7] undertook a preliminary economic study of geothermal desalination between 100 and 150 °C in Israel. Since 1990s, extensive research has been undertaken to utilise geothermal resources on the Cyclades Islands in Greece. This included the use of low-enthalpy (<100 °C) geothermal energy to power Multi-Effect-Distillation (MED) for seawater desalination on the islands of Milos [8,9] and Kimolos [10–13], with recent plans being reported for Nisyros [14]. On the Baja California Peninsula, Mexico, potential geothermal resources suitable for desalination have been discovered [15]. The utilisation of low- and medium-enthalpy sources is considered for seawater desalination using a tailored 20 m³/day MED design [16–18]. More recently, Oman planned to tap into the extensive low-enthalpy aquifer present in the Sultanate and the wider region for geothermal desalination [19]. Current research also includes the coupling of geothermal sources with the emerging Membrane Distillation (MD) [20,21], hybrid systems aiming toward polygeneration of water and energy [22], as well as the implementation of geothermal driven Reverse Osmosis (RO) systems [23,24].

* Corresponding author.

E-mail address: huitong.chua@uwa.edu.au (H.T. Chua).

Nomenclature

A	heat exchanger surface area (total), m^2
av	availability factor, –
C	cost (absolute), US\$, A\$
CPI	consumer price index, –
c	cost (specific), US\$/ m^3 , A\$/ m^3
d	distance, m
D	distillate production, m^3/day
f	friction factor, –
g	gravity, m/s^2
h	screen height, m
h_f	enthalpy, kJ/kg
hp	pumping power, hp
ΔH	head, m
i	interest rate, –
k	permeability, Darcy
L	piping length, m
μ	dynamic viscosity, $\text{Pa} \cdot \text{s}$, cP
\dot{m}	mass flow rate, kg/s
p	pressure, bar, Pa
PR	performance ratio, –
PR_{WH}	waste heat performance ratio, –
PHE	plate heat exchanger, –
Δp	pressure differential, bar, Pa
ψ	amortisation factor, –
r	radius, m
ρ	density, kg/m^3
S	skin factor, –
T	temperature, K, $^{\circ}\text{C}$
t	system lifetime, years
ΔT	temperature differential, $^{\circ}\text{C}$
\dot{V}	volumetric flow, kg/s
v	velocity, m/s
W_{elec}	electrical load, kW
<i>Subscripts</i>	
ad	additional
an	annual
$aqui$	aquifer at injection depth
CAP	capital expenditures (total)
cap	capital expenditures annualised
$cond$	condenser of the desalination plant
d	dynamic pressure drawdown
D	distillate
$DESAL$	desalination system
$elec$	electric power
ep	excess pressure in the geothermal production line
fl	friction loss
$fresh$	produced water
g	geothermal fluid
GEO	geothermal system
HS	heat source of the desalination plant
inj	injection well
in	inlet
$insurance$	insurance
$labour$	personnel
$maint$	maintenance
MED	multi-effect distillation plant
Mod	Modified MED system, e.g. Boosted MED
op	operation expenditures
PHE	plate heat exchanger
$prod$	production well
se	skin effect

sw	static wellhead
$treat$	pre-/posttreatment
ts	thermosiphon effect
w	well head

So far besides very general cost estimations for concrete applications [9,11,14,18,25,26], very limited research has been undertaken on detailed techno-economic analysis for the geographically more prevalent low-enthalpy ($<100\text{ }^{\circ}\text{C}$) systems [17,24]. Furthermore, where such studies had been undertaken, they were invariably focused on the above-ground infrastructure where the geothermal source was simply considered as a fixed source of energy for the matching of commercial desalination systems. Such an approach underestimates the full implications of geothermal desalination for two reasons.

- (1) In most cases, especially for deep low-enthalpy geothermal applications, the geothermal reservoir is not adequately characterised by a single pre-set point source. While its temperature can be fairly accurately predicted by the geothermal gradient, parameters like *permeability* and *transmissivity* of the aquifer can vary considerably with depths thereby impacting the operations and economics of the system. In fact, typically a system-specific optimum for the geothermal well field and the desalination plant exists, which requires both systems to be considered in tandem.
- (2) The cost structure of geothermal systems differs fundamentally from “conventional” energy sources. While typically the cost of energy occurs as operational expenditure by unit of *energy consumed*, in geothermal systems this cost is replaced by the large capital expenditures for the geothermal resource, e.g. exploration and provision of the wells/infrastructure. The cost of a geothermal system lies with the *provision* of hot geothermal fluid at the surface, which is almost independent of the extent of energy being extracted for downstream processes. For an economic operation of geothermal desalination systems a maximal energy extraction from the geothermal fluid is therefore favourable [27] and their performance should be measured by the *waste heat performance ratio* [28]. Established thermal desalination designs adopted from conventional applications are most often incapable of addressing this requirement sufficiently, thereby resulting in unit production rates far below the potential of the geothermal source [28,29].

This article aims to address these issues in the Western Australian context and provides tools to assess the potential of low-enthalpy geothermal resources for desalination in a more holistic way.

In addition, this article will show that by considering thermal desalination technologies tailored for low-grade heat sources, like *Boosted MED* (B-MED) [28–31] and *Preheated Boosted MED* (PB-MED), an improved utilisation of the geothermal resource can be realised, and significantly improve the economic prospects of the hydrothermal low-enthalpy geothermal desalination systems.

1.1. Hydrothermal, low-enthalpy geothermal desalination

This article focuses on the Hot Sedimentary Aquifer (HSA) geothermal reservoirs [32,33], which are prevalent in Australia.

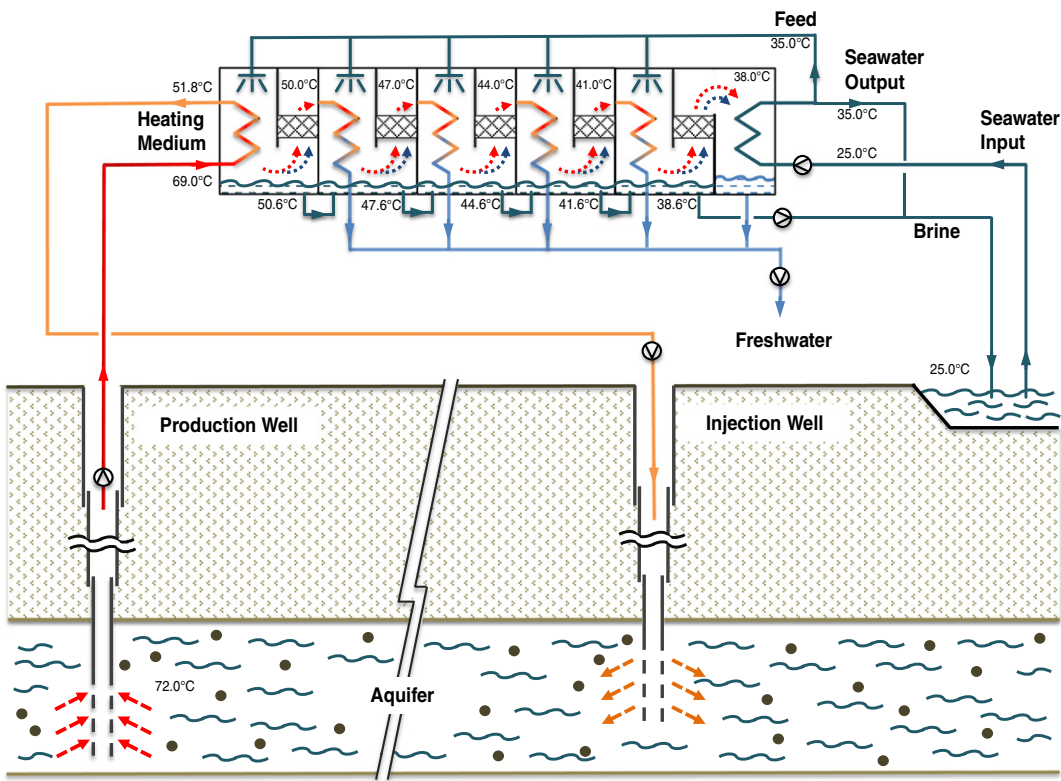


Fig. 1. Simplistic schematic of a low-enthalpy geothermal MED plant.

From these low-enthalpy sources, the hot geothermal fluid is extracted from the deep sedimentary aquifer and conveyed to the surface under pressure, so as to prevent the onset of precipitation. Heat is then harvested whereupon the colder geothermal fluid is re-injected into the aquifer [34,35]. The technology, reliability, economics, and environmental acceptability of such direct-heat geothermal applications have been widely demonstrated for district heating or heated swimming pools, especially in Western Australia [36].

Where sufficiently high reservoir temperatures are encountered, a conversion into mechanical work via Organic Rankine Cycles or Kalina processes is possible, which can be used to power RO units as demonstrated for example by Loutatidou and Arafat [24]. Stemming from the well known Carnot efficiency, however, the strong dependence of the conversion efficiency on the temperature differential between heat source and sink economically constrains these systems to a minimum temperature of about 100 °C. Operating at a reservoir temperature of 98 °C the Birdsville geothermal power station in Queensland, Australia, for example, achieves a heat use efficiency of 4% only [37]. In our context where a full re-injection of geothermal fluid is mandated, this can barely compensate for the full pumping power of the geothermal fluid, let alone supply power to a RO plant of practical capacity.

Hence at economically accessible depths with temperature levels below 100 °C, geothermal MED technology is offering a superior techno-economic solution.

Fig. 1 depicts a simplified schematic of a conventional geothermal driven MED system to treat saline surface water. Depending on the geochemistry, the system can either be directly heated by the geothermal water as shown in the figure, or indirectly via a secondary heating medium cycle or flashing process so as to manage scaling and contamination issues.

Novel variations of the MED process particularly designed for such low grade heat applications, like the *Boosted MED* (B-MED) as in Fig. 2,

have been developed that provide up to 30% more freshwater production over conventional MED systems [28].

A *Preheated Boosted MED* (PB-MED) is shown in Fig. 3, which by using two preheaters the heat source energy can be recovered further, while the production rate is increased as compared to both conventional and boosted MED systems. The impact of preheaters to improve the production rate of a conventional MED process has been widely discussed in [31]. With the same aim, we use preheaters to increase the production rate of the *Boosted MED* in this new layout (Fig. 3), while it is being coupled to a hydrothermal, low-enthalpy geothermal source. As shown in Fig. 3, the heat source outlet temperature is the lowest compared to both conventional and *Boosted MED* (Figs. 1 and 2) which is translated into a better utilisation of heat source energy (Appendix C). Synergistically the further cooling down of the heat source medium by means of the booster unit (in B-MED process) or additional preheaters (in PB-MED) can be manifested into a reduced re-injection depth and therefore considerably decreased well costs (refer to Section 2.2), provided that geological, geochemical, and environmental restrictions do not contradict such a reduction in re-injection depth.

The viability of the abovementioned novel processes layouts have been demonstrated via a pilot plant incorporating key features of the *Boosted MED* technology (Fig. 4), which shows a 57% additional vapour production in the downstream evaporator compared with that of the primary MED [30].

2. Techno-economic analysis of a low-enthalpy geothermal system

A holistic approach that considers the full implications of a geothermal resource toward minimising the levelised cost of water requires a coupled analysis of both the geothermal system and desalination plant subsections. The levelised cost of water can be

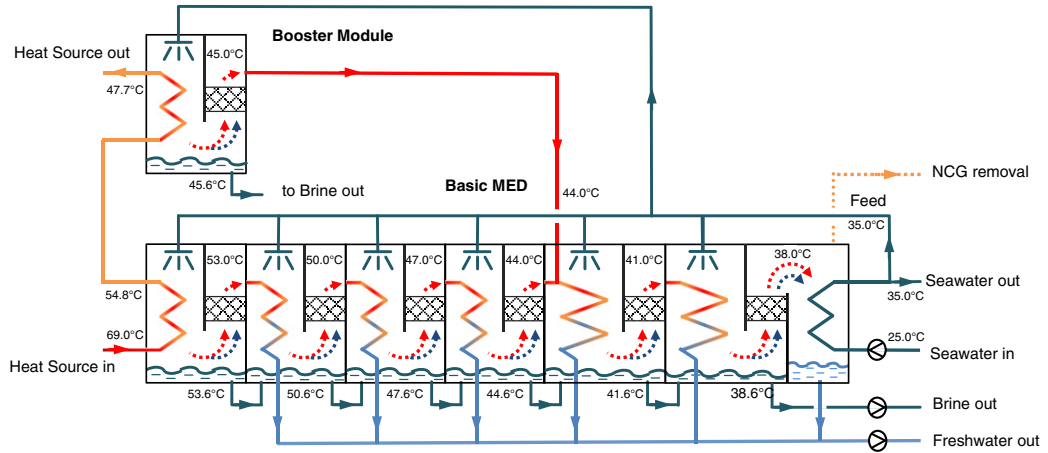


Fig. 2. The Boosted MED (B-MED) system tailored to geothermal heat sources, exemplary temperature distribution for a heating medium temperature of 69 °C.

expressed as the quotient of the total (annualised) costs, C_{an} , and the annual water production, D_{an} :

$$C_{fresh} = \frac{C_{an}}{D_{an}} = \frac{[C_{cap,DESAL} + C_{op,DESAL}] + [C_{cap,GEO} + C_{op,GEO}] + C_{insurance}}{av \cdot 365 \cdot D} \quad (1)$$

The techno-economic analysis is achieved by merging validated sub-models for each of the components into the global model, with further details about the economic integration of the parameters being provided below and in the [Appendix A](#).

2.1. Capital and operating expenditures of the desalination plant

A reliable approximation of the capital expenditure, $C_{cap,DESAL}$, of desalination plants is possible based on the GWI's Desalting Plant Inventory [38]. For conventional and *Boosted MED* plants up to a capacity of 10,000 m³/day, the following conservative cost functions, in US\$, can be applied, respectively [39].

$$C_{CAP,DESAL} = 3018.8 \cdot D_{MED}^{0.9795} \quad (2)$$

$$C_{CAP,Mod} = C_{CAP,MED} \left(0.31 + 0.4 \cdot \frac{A_{Mod}}{A_{MED}} + 0.29 \cdot \frac{D_{Mod}}{D_{MED}} \right) \quad (3)$$

However, for the *Preheated Boosted MED*, the price of preheaters which is estimated based on the functions below for grade 1 titanium plate heat exchangers [40,41] is added to the relevant *Boosted MED* capital cost function and adjusted by the producer price index.

$$C_{CAP,PHE} = 131 \cdot A_{PHE}^{0.7514}; (A_{PHE} > 200 \text{ ft}^2) \quad (4)$$

$$C_{CAP,PHE} = 612 \cdot A_{PHE}^{0.4631}; (A_{PHE} < 200 \text{ ft}^2) \quad (5)$$

The sizing and pressure drop calculations of those preheaters follow the prescriptions of Polley and Haslego [40] and constrained by a maximum heating medium pressure drop of 5 m as per [Table B.2](#).

The annualised capital cost of the desalination plant results from the amortisation factor, ψ .

$$C_{CAP,DESAL} = C_{CAP,Mod} \cdot \psi = C_{CAP,Mod} \cdot \frac{i \cdot (1 + i)^t}{(1 + i)^t - 1} \quad (6)$$

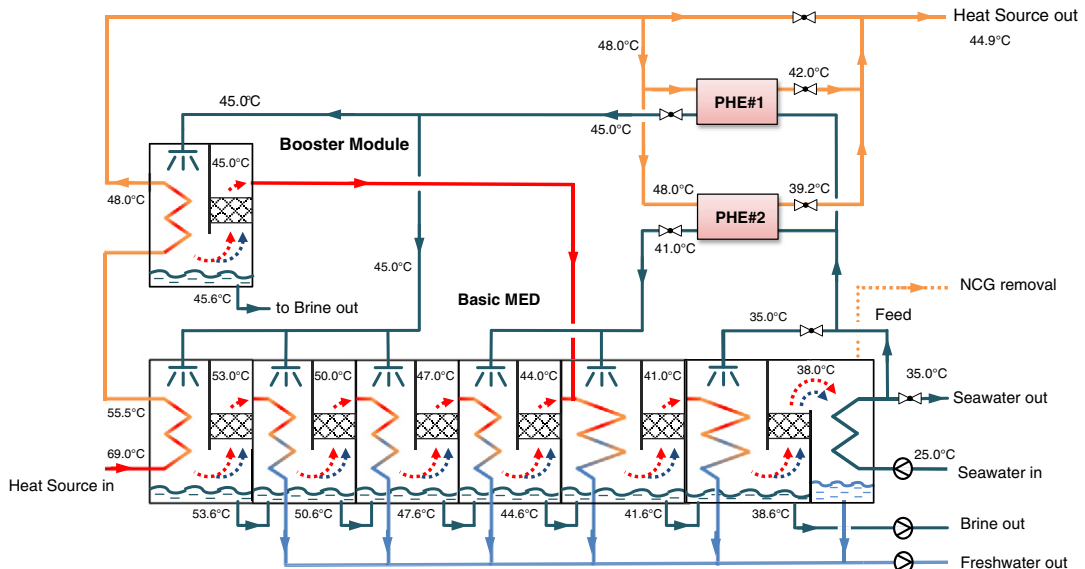


Fig. 3. The Preheated Boosted MED (PB-MED) system tailored to geothermal heat sources, exemplary temperature distribution for a heating medium temperature of 69 °C is presented.



Fig. 4. Photograph of the pilot plant at the National Centre of Excellence in Desalination Australia Lab, Rockingham, Western Australia.

The annual operational costs of the desalination plant can be determined by considering the expenses for personnel, C_{labour} , auxiliary power consumption, $w_{elec,DESAL}$, electricity cost, C_{elec} pre and post treatment, C_{treat} , and operation and maintenance, $C_{mant,DESAL}$:

$$C_{op,DESAL} = D_{an} \cdot (w_{elec,DESAL} \cdot C_{elec} + \sum C_{treat} + C_{mant,DESAL}) + \sum C_{labour} \quad (7)$$

2.2. Expenditures of the geothermal system

2.2.1. Capital expenditures of the geothermal system, $C_{cap,GEO}$

A major aspect in the economic feasibility of deep geothermal systems is related to the development of the geothermal well field. Due to the infancy of the industry and the geological uncertainty associated with drilling at specific sites, ascertaining these well costs tend to be very challenging [41].

Besides technical reasons, e.g. varying diameters, lithology, unplanned events occurred during the well preparation process [42], the prevailing situation of the oil and gas market, availability of drilling rigs as well as geographical position of the well field are regarded as main drivers [43]. Importantly, in areas where advantageous geological conditions require only drilling depths shallower than 2000 m, smaller drilling rigs commonly used for water wells may be used. This can significantly reduce drilling costs to as low as 1000 US\$ per meter [41,44].

The annualised capital cost of the geothermal well field, following from Eq. (6), can be expressed as:

$$C_{cap,GEO} = C_{CAP,GEO} \cdot \psi = C_{CAP,GEO} \cdot \frac{i \cdot (1+i)^t}{(1+i)^t - 1} \quad (8)$$

The actual required well depth is determined by the average temperature of the aquifer at extraction depth. In conduction dominated reservoirs, this temperature can be estimated by the local average geothermal gradient. Where advantageous fluid flows are present, significantly increased temperatures can be encountered [45,46], thereby significantly reducing the required well depth.

Inevitably, the hot geothermal fluid has to pass colder layers en route to the surface, thereby resulting in heat losses along the well. As an approximation, the losses can be considered as a fixed depth related value as shown in Table 1.

Also, further capital expenditures related to the geothermal system, including the production and reinjection pumps [47,48] and the infrastructure preparation, which is location and application dependent, need to be considered. Exemplary figures are also included in Table 1.

Table 1
Geothermal parameters.

Geothermal target temperature	As per Fig. 8
Permeability at target depth	As per Fig. 8
Flow rate of geothermal fluid	100
Salinity of geothermal fluid [71]	-15,000 ppm
Potentiometric height	-5 m
Production/injection wells	
Temperature drop due to heat losses along the well	2 °C/km
Casing	14"/12" strings of equal length
Screen height, h	250 m
Skin factor, S	1 [-]
Depth of submersible pump	250 m
Efficiency of the submersible pump	0.72 [-]
Efficiency of the injection pump	0.80 [-]
Pressure drop of heat exchangers	0.5 bar/each
Overpressure for degassing/precipitation prevention	5 bar
CAPEX of geothermal wells	1300 AUD/m
Additional expenditures for well field development	500,000 AUD
CAPEX of production pumps ^a	12,434 · (hp) ^{0.5} AUD
CAPEX of injection pumps ^a	892 · (hp) AUD
Lifetime of geothermal pumps	15 years
Maintenance of well field (% of CAPEX of well field)	1 [-]

^a [47,48], producer price index adjusted [77].

2.2.2. Operational expenditures of the geothermal system, $C_{op,GEO}$

The major operational expenditures of deep Hot Sedimentary Aquifer geothermal systems pertain to the energy required to pump the geothermal fluid to the surface and the subsequent reinjection into the aquifer. This auxiliary power, $w_{elec,GEO}$, is heavily dependent on the characteristics of the well field and may render an otherwise promising project uneconomical. Fig. 5 shows the sensitivity of the auxiliary pumping power as a function of the permeability of the reservoir based on the existing “Cockburn 1” well located in the Perth Metropolitan Area, Australia.

The conventional practice of assuming pre-set, fixed well field parameters (or even “typical” pumping power data as adopted from different projects) commonly found in techno-economic studies for geothermal desalination is very prone to erroneous estimates for the pumping power, potentially putting the entire project at risk.

In this paper, we have included this crucial auxiliary pumping power in our analyses. This has been done by adopting a facile hydrogeological pumping model [35,41,49,50]. For the present example in Western Australia, the model has been validated against operational data to within $\pm 10\%$ from a local geothermal system (Fig. A.2). The detailed validation can be found in Appendix A.

In this model, in addition to assuming a homogeneous permeability of the aquifer, we assume a horizontally isothermal behaviour, and neglect variations of the aquifer temperature over the well lifetime by applying an average temperature profile.

The wellhead pressure p_w that determines the pumping data for the production pump can be expressed as [35]

$$p_{w,prod} = p_{sw} + \Delta p_d + \Delta p_{se} + \Delta p_{fl} + \Delta p_{ad} + \Delta p_{ep} \quad (9)$$

and for the injection pump as

$$p_{w,inj} = p_{sw} + \Delta p_d + \Delta p_{se} + \Delta p_{fl} - \Delta p_{ts} \quad (10)$$

with $p_{sw} = \Delta H \cdot \rho_g \cdot g / 10^5$ being the static wellhead pressure [bar] where ΔH is the differential height of the water level [m], ρ_g the density of the geothermal fluid [kg/m^3], and g the gravity [m/s^2].

Δp_d represents the dynamic pressure drawdown of the reservoir. In applications involving the re-injection of the brine, or where a continuous recharge of the reservoir is provided so that the pressure can remain

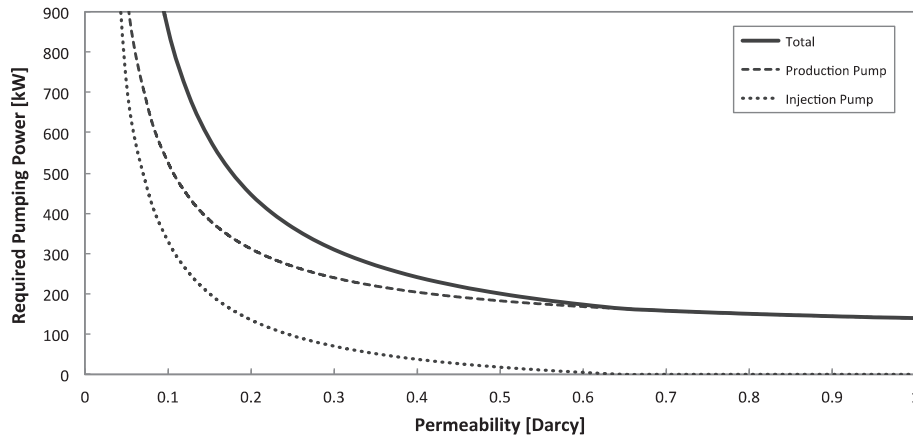


Fig. 5. Predicted pumping power as a function of permeability at a target temperature of 75 °C, based on data from the “Cockburn 1” well, Perth Metropolitan Area, Western Australia (detailed data are provided in [Appendix A](#)).

stable, the steady state reservoir dynamic pressure drawdown is given as [35]

$$\Delta p_d = \frac{\dot{V}_g \cdot \mu_g}{k \cdot h} \cdot \log_{10} \left(\frac{d}{r_B} \right) \quad (11)$$

where \dot{V}_g is the volumetric flow rate of the geothermal fluid, μ_g the dynamic viscosity of the geothermal fluid in [cP], k the intrinsic permeability of the reservoir [Darcy], h the penetrated aquifer height, r_B the well radius at reservoir and d the distance between the production and injection wells [m].

The skin effect pressure drawdown Δp_{se} considers effects occurring at the well-reservoir interface induced by either formation impairment (positive skin) or upgrading (negative skin).

$$\Delta p_{se} = 0.44 \frac{\dot{V}_g \cdot \mu_g \cdot S}{k \cdot h} \quad (12)$$

The friction losses, Δp_{fl} , of the casing strings, bends, etc. are calculated as per standard internal flow within conduit,

$$\Delta p_{fl} = f \cdot \left(\frac{L}{2r} \right) \cdot \left(\frac{\rho \cdot v^2}{2} \right) \quad (13)$$

where L is the length of the casing section, $2r$ the hydraulic diameter of the pipe, and v the mean flow velocity.

The additional pressure losses, Δp_{ad} , consider all additional pressure drops in the aboveground process, as induced for example by heat exchangers and control devices, etc.

Δp_{ep} considers the requisite excess pressure within the piping system in order to maintain a stable operation as well as to avoid excessive degassing and precipitation from the geothermal fluid.

Whenever the temperature of the re-injected fluid is lower than the aquifer temperature at the reinjection depth, the density differential assists the pumping process as ordained by the thermosiphon effect or Δp_{ts} [35]

$$\Delta p_{ts} = g \cdot (\rho_{g,inj} - \rho_{g,aqui}) \cdot H_{A,inj} \quad (14)$$

The properties of the geothermal fluid are approximated as a function of temperature and salinity according to [51].

Additional operational costs of the geothermal wells are included as maintenance cost, $C_{mant,GEO}$. While the wells demand only minimal care during regular operation, over the lifetime of the field unexpected issues can arise that can involve costly treatment (e.g. scaling or corrosion of the casing [32,35]). To cover such possibilities, we consider 1% of the

capital costs of the wells annually [52]. The main consideration here is to ensure that the aboveground geothermal loop is leak free, since any oxygen ingress or pressure drop may cause fouling and extra maintenance. To this end, we consider an aboveground overpressure of 5 bar as in [Table 1](#) below. While the operation conditions can be variable, it is a good practice to factor in maintenance operations every seven years such as air lifting scalings on the drillhole screens and back flushing the heat exchanger. This can be monitored by the pumping pressure requirement.

Consequently, the total operational expenditures of the geothermal system can be expressed as:

$$C_{op,GEO} = 8760 \cdot av \cdot \sum w_{elec,GEO} \cdot C_{elec} + C_{mant,GEO} \quad (15)$$

2.3. Expected production rate of the MED plant

The expected freshwater production rate, as well as the required heat exchanger surface area used for the capital cost estimation, are based on the detailed and validated thermodynamic optimisation model introduced in detail in [\[30,31\]](#). For this model, which is partly adopted from El-Dessouky and Ettouney et al. [53–55] and has been validated against operational data from the pilot plant [30], the following standard engineering approximations are applied [56]:

- Steady state operation.
- Distillate is pure water.
- No sub-cooling of the distillate occurs in the effects.
- Losses due to Non-Equilibrium Allowance (NEA) and pressure drops from the demister etc. are negligible.
- Energy losses to the environment are negligible.

For the optimisation of geothermal heat applications, only the cooling water temperature, feed salinity, minimal allowable temperature differential over the effects, top brine temperature and recovery ratio are used as input parameters. The temperature, specific heat capacity and available mass flow rate of the heating medium input and output temperature are considered in tandem with the geothermal module, whereas for example the number of effects, and temperature gradient across the effects remain as independent variables.

3. Exemplary techno-economic analysis for Western Australia

Based on these considerations the techno-economic analysis is performed for Western Australia. As reference for the economic data like

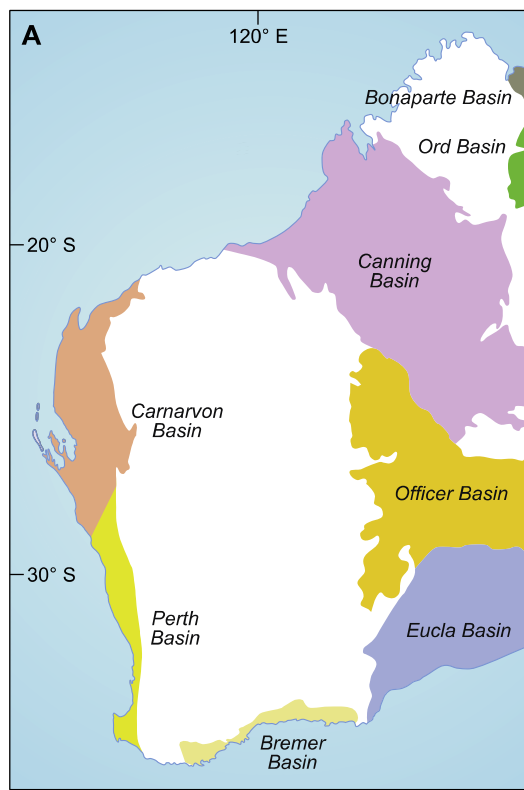


Fig. 6. Onshore sedimentary basins in Western Australia [57].

exchange rates, producer price indices, etc. the year 2013 is used, which is the year the project, which this analysis is part thereof, started.

3.1. Geothermal potential

In Western Australia, there are eight sedimentary basins with on-shore components (Fig. 6), of which the Canning, Carnarvon, Officer and Perth Basins are deep enough to have temperatures above 60 °C [57].

Geothermal investigations that have been performed in this area since 1950s [37,57–66] conclude that higher temperature applications are viable in the North Perth Basin and Western Canning Basin, while good reservoir properties for low-enthalpy applications requiring high flow rates are also found in the South Perth Basin, Carnarvon Basin, Officer Basin, and Western Canning Basin. Fig. 7 juxtaposes the geothermal prospects across Western Australia with local population densities.

We undertake an exemplar case study in the Northern Perth Basin for the regional Centre of Geraldton. The City of Geraldton is located 400 km north of Perth and has a population of around 37,000 [67]. It borders between a Mediterranean and semi-arid climate [68]. A substantial portion of the city's water demand is covered by groundwater bores screened in the shallower areas of the Yarragadee Formation, at about 50 km south of the city and near the town of Dongarra [69]. These well fields service also the water supply of the nearby towns of Port Denison, Walkaway, Dongarra, and Narngulu [70]. The population increase in this region is well over the Australian average, and for Geraldton a potentially doubling in population is anticipated until 2020 [67,69]. Beside the significant increase in demand, relatively high bore water salinities with a temporal increasing tendency due to saltwater intrusions is a major water issue [69].

Fig. 8 depicts the borehole temperatures and measured permeabilities of several wells in the broader area within the North Perth Basin where the region concerned is located. Generally good reservoir

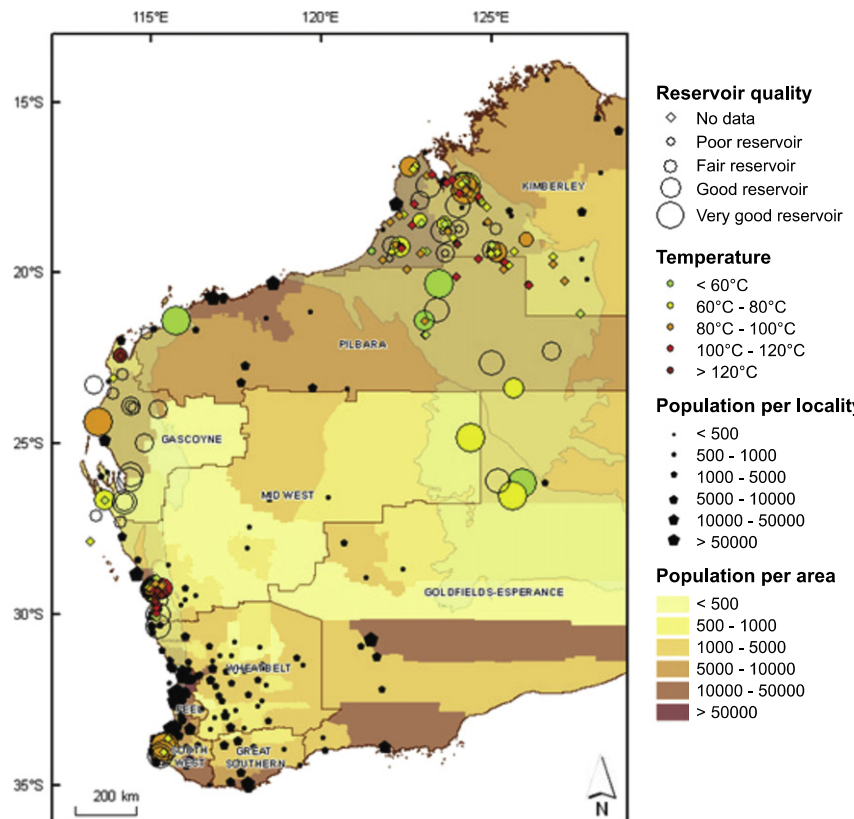


Fig. 7. Geothermal prospects across Western Australia [57].

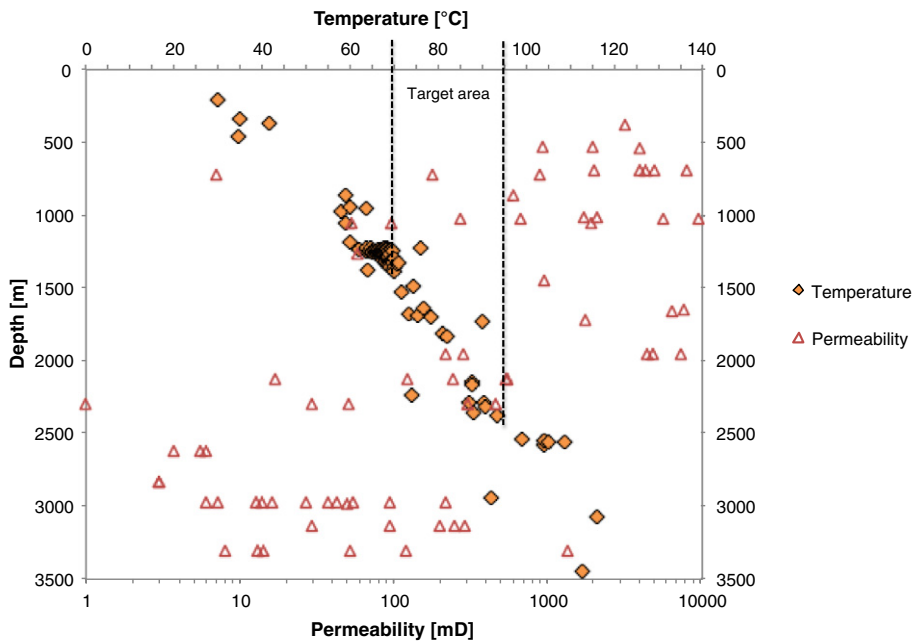


Fig. 8. Borehole temperatures and permeabilities in the Yarragadee formation of the North Perth Basin, data adapted from [71].

qualities have been reported in this area; but the co-location of highly permeable rocks and reservoir or rock formation at which high temperatures are measured is somewhat uncertain [57]. Also some uncertainty is typically associated with the borehole temperatures. However the available data do provide a very good estimation of the geothermal parameters needed.

On account of the relatively high salinities as per Table 1 below, SS316 is typically selected as the casing material for the wells.

3.2. Input parameter

Due to various reasons, including high wages, and geographical remoteness, several cost parameters stemming from generic global datasets have to be adjusted to reflect the local conditions:

3.2.1. Well field development

There are no deep geothermal wells in Western Australia and only a very small number of suitable rotary rigs have been employed in Australia [72]. For projects outside the major metropolitan areas, the well field development cost using conventional rigs employed in the oil and gas industry is estimated to be three times that of the international average. Among other reasons, this is due to the competing demand from the oil and gas sites of those suitable rigs that are already low in supply [72].

Alternatively, locally available smaller rigs, typically used for water wells and shallower geothermal projects can offer a solution for this issue, provided the regulatory framework is addressed. Technically, some of the rigs are capable of drilling at the present lithology to as deep as 2000 m [44]. Based on experience with shallower geothermal projects in the Perth Metropolitan Area, well costs for these systems are estimated at 1300 AUD per meter [41,44]. This is the technology that we are adopting in this study.

3.2.2. Desalination plant

A similar situation applies to the capital expenditures of desalination plants. The capital costs of recent large scale RO plants in Australia have been two to four times above the estimations based on international data [73]. A number of factors have been cited for this escalating cost [73,74], including: (1) The emergency response nature of most Australian municipal SWRO projects resulting in 'crisis prices' for the construction of those plants, (2) The political imperative to offset at

least part of the carbon footprint by acquiring Renewable Energy Credits equivalent to the power consumption of the plant thereby involving additional capital expenditure, and (3) relatively high wage rates for desalination project construction workers in Australia. Apart from the high wage rates, which is by far the most important factor, most of these issues, only partially apply to smaller sized (up to $\sim 5000 \text{ m}^3/\text{day}$), renewable energy driven systems, thereby resulting in an escalation factor that is far more subdued than those encountered in large RO plants for these significantly smaller MED units. A larger degree of prefabrication and standardisation can therefore be expected, thereby dampening the magnitude of increase. Consequently, an estimated increase of 20% above the global average has been considered for the capital cost of the MED plants in this study. This has been independently benchmarked against quotations solicited in-confidence from reputable suppliers.

3.2.3. Labour cost

The average annual cost for a skilled employee in the water industry in Australia is 97,900 AUD/year [75]. For remote locations and applications proximate to mine sites, employment costs well above the Australian average can be expected.

3.2.4. Electric power

The Australian electricity prices are among the highest in developed countries [76]. Areas without access to the power grid have to endure even significantly higher electricity costs and/or load limitations.

Table 2

Desalination parameters.

Seawater temperature [78]	25	°C
Seawater salinity [79]	35,500	ppm
Specific heat of geothermal fluid	4.2	kJ/kg K
Recovery ratio	0.35	[—]
Maximum ΔT of cooling water	10	°C
Maximum top-brine-temperature	70	°C
Minimum ΔT of heat exchanger	3	°C
Pressure difference for steam injection, Δp , in B-MED and PB-MED	500	Pa
Maintenance [80,81]	0.04	AUD/m ³
Chemicals (pretreatment/potabilisation) [55,81]	0.02	AUD/m ³

Table 3
Economic considerations.

Plant lifetime [81]	30	years
Plant availability [81]	98	%
Electrical power cost [82]	0.151	AUD/kWh
Labour cost [75]	98,000	AUD/employee
Insurance (annual premium of total CAPEX)	0.25	%
Interest rate	7	%
Exchange rate US\$/AUD [83]	1 US\$ = 1 AUD	

3.3. General input parameters

As general input parameters for the analysis, the data as presented in Tables 1 to 3 have been considered.

3.4. Results

Based on the above parameters and the geothermal parameters as in Fig. 8, the estimated water costs for different target depths, viz. 1500 m, 1800 m and 2200 m derived from the techno-economic model are presented in Table 4.

The estimated cost of water ranges from 2.60 AUD/m³ for the shallower depths characterised by higher permeabilities, to 1.89 AUD/m³ at around 1800 m. Due to the decrease in permeability, deeper systems again show an increasing cost of water, rendering systems deeper than 2200 m not realistic at this location. The comparison between conventional MED and the *Preheated Boosted MED* (PB-MED) systems reveals that the latter can reduce the levelised cost of water by 16% over the surveyed application range. The same comparison between the PB-MED and B-MED over the surveyed application range shows a 5% reduction in the levelised cost of water. The additional initial investment for both B-MED and PB-MED systems is higher than the conventional MED plant, mainly due to the additional booster effect and heat exchanger surface area. However as a whole both systems reduce the water price significantly.

The main drivers for this cost reduction by the *Boosted* and *Preheated Boosted MED* are (1) the increased freshwater yield stemming from the improved utilisation of the geothermal fluid and (2) reduced well field expenses due to a shallower re-injection well.

Over the examined application range for the regional Centre of Geraldton, the *Preheated Boosted MED* system as applied to a well field with an 1800 m deep production well is the most economic configuration. This configuration is therefore used as the basis for further parametric studies.

Fig. 9 shows a breakdown of the various costs for both conventional and *Preheated Boosted MED* systems. The geothermal system related expenditures (CAPEX and OPEX) contribute approximately 45% to the final water cost. This is well within the typical range of energy related cost contribution to conventional desalination systems. One major difference however is that in contrast to conventional fossil fuel driven systems, where the energy costs primarily occur as ongoing fuel/energy expenditures, in the geothermal systems over 50% of that share incurs upfront.

The largest uncertainties of this base case scenario are related to the geothermal parameters, in particular the flow rate and the reservoir permeability. In the absence of exact data for these parameters prior to the well field development, only estimations are possible. Fig. 10 illustrates the respective impact of permeability and flow rate on water cost for the three systems.

The flow rate of the hot geothermal fluid is linearly related to the extractable energy at the surface. Within the application range the well costs are predominantly a function of well depth, rather than well diameter. Lower geothermal flow rates translate directly to a reduced freshwater production at an ostensibly unaltered capital cost. The immediate consequence is an increased specific water cost, as encountered in Fig. 10. This correlation is of particular interest, as in fact most often the actual geothermal flow rates remains unknown until a relatively late project stage of the well field development.

A similar situation applies to the permeability, which is directly related to the pumping costs for the geothermal system. At permeabilities beyond 0.3 Darcy, its influence on the overall water costs remains relatively stable. However, where lower permeabilities are encountered, the exponentially increasing power consumption enjoins a corresponding rise in operational cost for the well system, and consequently escalating water costs.

Fig. 11 depicts the sensitivity of further key parameters on the specific water cost in relation to the base case scenario. Besides the influence of flow rate, permeability, and geothermal gradient, the water

Table 4
Results for different target depths – MED, B-MED and PB-MED.

Target depth	1500 m			1800 m			2200 m		
	MED	B-MED	PB-MED	MED	B-MED	PB-MED	MED	B-MED	PB-MED
Geothermal well field									
Production well (km)	1500	1500	1500	1800	1800	1800	2200	2200	2200
CAPEX (10 ⁶ A\$)	1.95	1.95	1.95	2.34	2.34	2.34	2.86	2.86	2.86
Injection well (m)	920	800	800	1010	810	800	1090	890	800
CAPEX (10 ⁶ A\$)	1.19	1.04	1.04	1.31	1.06	1.04	1.41	1.16	1.04
Additional cost of well field development (10 ⁶ A\$)	0.50	0.50	0.50	0.50	0.50	0.50	0.50	0.50	0.50
Geothermal pumps (10 ⁶ A\$)	0.17	0.17	0.17	0.21	0.22	0.23	0.34	0.36	0.39
Pumping power of geothermal pumps (kW)	133	140	147	179	195	209	323	350	378
Maintenance of geothermal well field (10 ³ A\$/year)	31	30	30	36	34	34	43	40	39
Desalination plant									
Freshwater production (m ³ /day)	1110	1340	1470	1710	2030	2270	2200	2550	2870
Freshwater production (10 ³ m ³ /year)	397	478	525	611	726	812	788	912	1026
CAPEX (10 ⁶ A\$)	3.48	4.00	4.30	5.31	6.02	6.61	6.81	7.58	8.38
Chemicals (10 ³ A\$/year)	9	11	12	13	16	18	17	20	23
Labour (10 ³ A\$/year)	98	98	98	98	98	98	98	98	98
Maintenance (10 ³ A\$/year)	16	19	21	24	29	32	32	36	41
Auxiliary electricity cost (10 ³ A\$/year)	95	115	129	129	160	184	166	194	225
Insurance premium (10 ³ A\$/year)	18	19	20	24	25	27	30	31	33
Discount rate (%)	7	7	7	7	7	7	7	7	7
Plant lifetime (years)	30	30	30	30	30	30	30	30	30
Levelised cost of water (A\$/m ³)	2.60	2.29	2.19	2.20	1.98	1.89	2.25	2.07	1.97

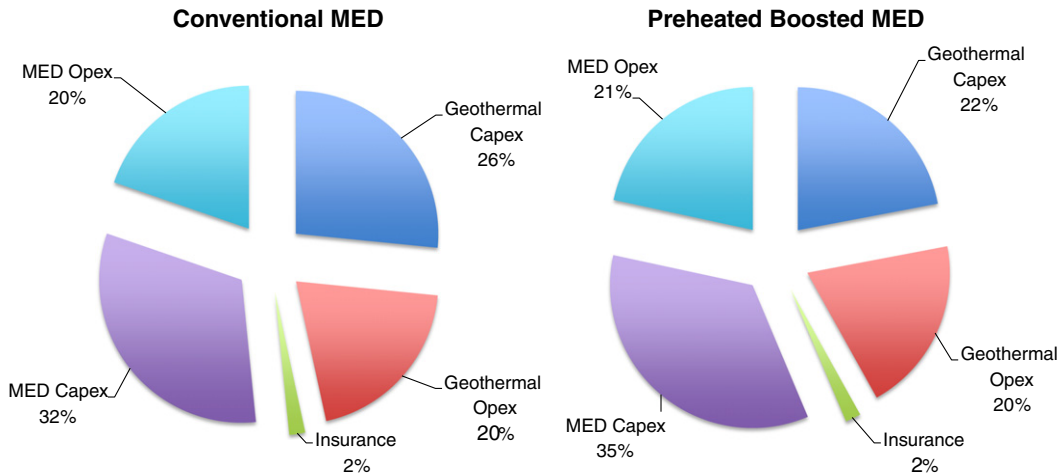


Fig. 9. Water cost breakdown for *Conventional* and *Preheated Boosted MED* systems, 1800 m target depth, (base case scenario).

price is expectedly very sensitive to the well field completion costs. Importantly due to the relatively high capital cost component, the specific water cost is very sensitive to the discount rate. This is particularly important for the cross-comparison with other published cost estimates, as a broad range of discount rates can be found in the literature (Table 5).

3.5. Discussion

Regarding the specific water costs, these figures have to be meaningfully benchmarked against those of alternative water sources, and other desalination systems.

A reasonable comparison with alternative sources of water can be achieved by the current direct water costs in the area. Beyond the water scheme supplying the Perth Metropolitan Area and nearby regions, including the Goldfields, very high water costs can be encountered. Especially for remote and often smaller communities, water costs over 6 AUD/m³ and even in excess of 25 AUD/m³ have been reported [84,85] (Fig. 12).

The actual direct water production costs are not generally disclosed from the supply companies and due to the regulated water pricing structure, no direct relation between the actual local production costs and the water price can be drawn. The latest publicly available data for Geraldton and Dongarra, dating from 2006, however reveal a local direct cost of 1.45 AUD/m³ [85]. Depending on the applied consumer price index, this would translate to 1.76 AUD/m³ (Perth specific CPI) or 2.61 AUD/m³ (Australian water supply and sewage specific CPI) in the reference year 2013.

Table 6 lists a collection of Australian specific water costs of various desalination technologies for comparison, while **Table 7** provides an overview of some cost estimates of renewable energy driven desalination technologies.

Comparing the results of the techno-economic model on a general scale against the levelised cost of alternative renewable energy driven desalination technologies (Table 7), the surveyed geothermal desalination based on the *Preheated Boosted MED* is well within an economically competitive range. Depending on the local geological conditions, it can therefore represent the most favourable, renewable energy driven freshwater supply. For the present case study, for example, with levelised cost

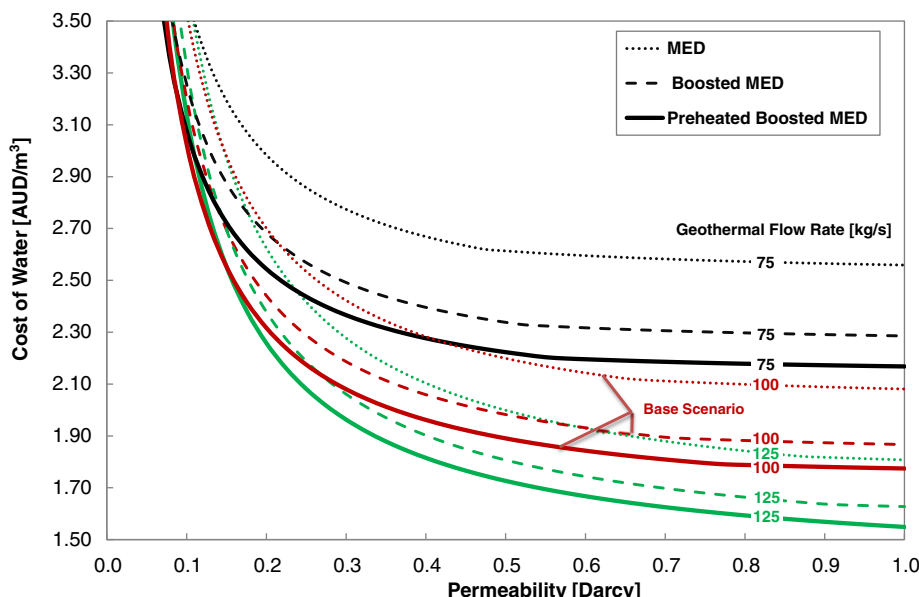


Fig. 10. Influence of the permeability and the geothermal flow rate on the estimated cost of water, 1800 m target depth.

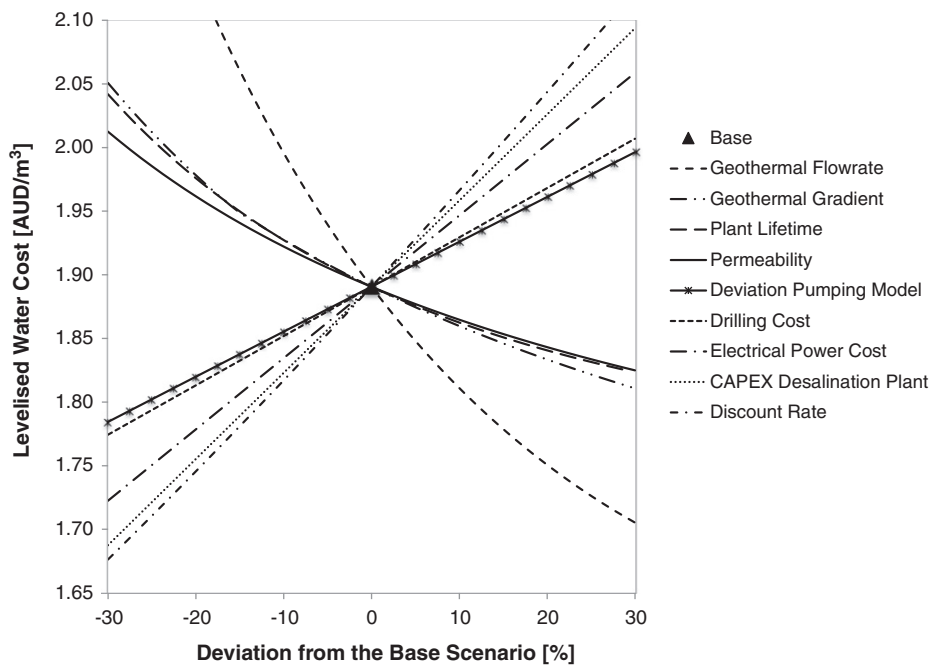


Fig. 11. Influence of various parameters on the levelised water cost of the *Preheated Boosted MED* system, at 1800 m target depth.

Table 5
Effect of discount rate on the specific cost of water.

Target depth [m]	Geothermal flow rate [kg/s]	MED			Boosted MED			Preheated Boosted MED		
		Discount rate			Discount rate			Discount rate		
		5%	7%	9%	5%	7%	9%	5%	7%	9%
1800	75	2.29	2.61	2.96	2.05	2.34	2.65	1.95	2.22	2.52
	100	1.95	2.20	2.46	1.77	1.98	2.22	1.69	1.89	2.11
	125	1.80	2.00	2.21	1.63	1.81	1.99	1.56	1.73	1.90

of water in the range of 2.00 AUD per m^3 , the application of the Preheated Boosted MED at around 1800 m depth provides an economically and technically viable freshwater supply solution with a low environmental impact.

4. Conclusion

A techno-economic analysis that explicitly includes the sub-surface system has been undertaken to assess the potential of low-enthalpy geothermal resources for desalination in Western Australia. Simulation modules validated by actual experimental data via a local geothermal system and a *Boosted MED* pilot plant were integrated to arrive at a robust analysis.

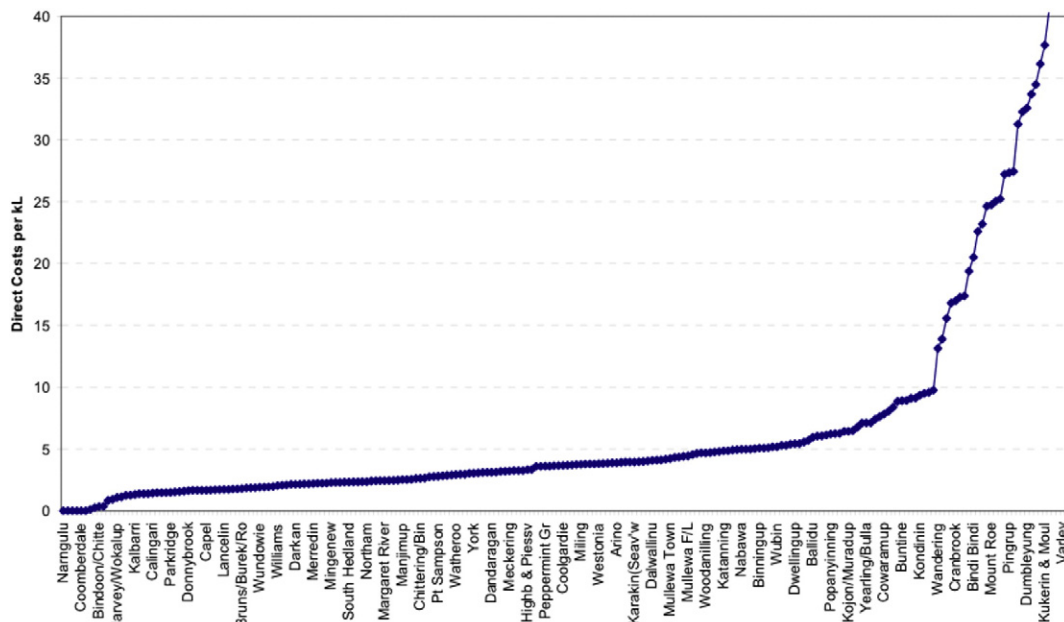


Fig. 12. Cost of production for rural drinking water in Western Australia [85].

Table 6

Published cost of water of various desalination technologies – Australia specific.

	Plant capacity [m ³ /day]	Unit cost [AUD/m ³]
MED	300	0.90/2.70 ^a
	1000	0.60/2.00 ^a
RO	5–50	1.89–2.20 ^b
	>10	<1.25–2.00 ^c
MED	180–265	4.00–6.5 ^d
	200	2.21 ^e
	10,000	1.17 ^f
MSF	10,000	1.97 ^f
RO	10,000	0.95 ^f
	140,000–250,000	1.19–1.44 ^g
	153,000	2.20 ^g

^a [86], estimated costs, with/without waste heat utilisation.^b [86] estimated costs.^c [87], data from 46 Australian desalination plants (SWRO and BWRO), <1.25 AUD/m³ for portable water, 1.25–2.00 AUD/m³ for product water.^d [84], data from 3 small scale BWRO and SWRO plants in Western Australia.^e [88], groundwater RO, estimated cost.^f [89], estimations for Australia based on cost database.^g [90] [91], actual data from large scale Australian RO plants.**Table 7**

Published cost of water of various renewable energy driven desalination technologies – general.

	Plant capacity [m ³ /day]	Unit cost [US\$/m ³]
Renewable energies		
Hybrid RO (grid-wind)	3–120	3.87–11.61 ^{a,f}
Hybrid VC (grid-wind)	1200	1.95 ^{b,f}
Solar thermal	1200	2.46 ^{b,f}
Wind VC	Not specified	0.87–5.48 ^c
Wind RO	Not specified	2.13–2.44 ^c
Wind	Not specified	1.5–1.77 ^c
Photovoltaic	Not specified	1.29–6.45 ^{d,f}
Solar collectors	Not specified	4.05–11.61 ^{d,f}
Geothermal	30,000	4.51–10.32 ^{d,f}
		2.06/2.48 ^e

^a [92], actual data, including solar MED, geothermal MED, MVC, PV-RO, Wind-RO, and hybrid RO (Wind-PV).^b [93], case study.^c [84], compiled from various sources, not specified by the author.^d [94], review and assessment of water desalination cost literature.^e [24], case study, geothermal driven RO and MED.^f 1 EUR = 1.29 USD (www.xe.com, 18.03.2013).

For the surveyed application in the Western Australia Northern Perth Basin, it is demonstrated that competitive levelised water costs on the order of 1.56 to 2.52 A\$/m³ can be achieved. A comparison among conventional MED, the *Boosted MED* and the *Preheated Boosted MED* technology highlights the importance of maintaining an increased energy extraction from the geothermal source, thereby resulting in a reduction of the levelised unit cost on the order of 13 to 16%.

Over the surveyed application range (namely 1500, 1800 and 2200 m as target depths), a location specific optimal target depth exists at 1800 m, where the geothermal parameters, namely wellhead temperature and permeability, provide the economically best match to the desalination system. The levelised cost of water at this target depth is in the range of 5 to 15% lower in comparison with the other surveyed target depths for all the considered desalination technologies, namely, MED, B-MED and PB-MED. Concomitantly, at this condition, the geothermal-system related expenditures (capital and operational) contribute approximately 45% to the final water cost, which is well within the typical range of energy related cost contribution to conventional desalination systems. In this scenario, the PB-MED results in the lowest levelised cost of water (1.89 A\$/m³) among the various technologies. In addition the pivotal importance of the geothermal fluid flow rate has been identified and shown that an increment of around 67% in the geothermal fluid flow rate (from 75 to 125 kg/s) reduces the levelised

cost of water by 20 to 25% for the various considered discount rates and applies equally to all of the considered desalination technologies.

Benchmarked against both the levelised cost of water for existing sources and alternative desalination technologies, geothermal desalination based on both *Boosted* and *Preheated Boosted MED* technologies can provide an economically and technically viable freshwater supply solution with a small environmental footprint.

Acknowledgement

We gratefully acknowledge the financial support from the University of Western Australia and the National Centre of Excellence in Desalination Australia, which is funded by the Australian Government through the National Urban Water and Desalination Plan. We also acknowledge the support of Mr. Jaxon Smeed, who collected the data used for the validation of the geothermal pumping model.

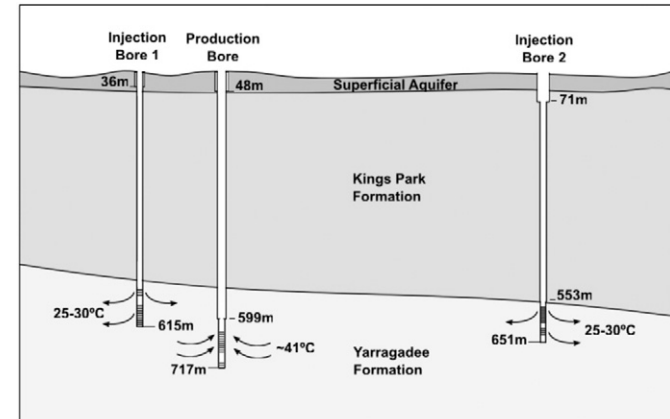
Appendix A. Validation of the hydrogeological pumping model

The pumping model is validated based on data collected from the largest low temperature geothermal heating system in Australia, located at the HBF Stadium, known previously as the Perth Challenge Stadium [95].

The HBF Stadium is the biggest purpose built outdoor aquatic centre in the Southern Hemisphere. A geothermal system is utilised to heat its three outdoor and two indoor pools with a total water volume of 11 million litres, as well as to preheat the changing room showers [36,95].

The geothermal system of the HBF Stadium accesses ~41 °C hot geothermal fluid in the Yarragadee Formation – the same formation within the same Perth Basin which the present case study is targeting. This hot water is passed through separate heat exchangers for the different pools/showers, and returned at ~25–30 °C into the aquifer. Fig. A.1 depicts a schematic of the well field. A variable speed pump is installed to maintain the requisite flow rate, so as to track the heating requirements of the different pools.

Fig. A.1 Schematic of the HBF Stadium well field, based on [95,96].



To validate the pumping model, system operational data were collected at varying operational modes. The volumetric flow rate, input and output temperatures, differential pressure of the aboveground system, and the actual pumping load of the variable speed pumps were logged in fifteen-minute intervals. The system design parameters were gleaned from the system manual [96], and supplementary geological information was obtained from the proximate St. Hilda's Anglican School for Girls well field (Table A.1).

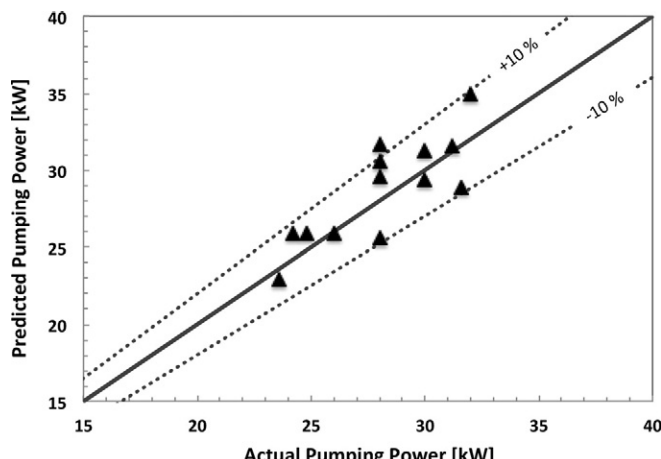
The actual operational flow rate ranged between 8 and 25 l/s, with a typical operational range between 14 and 18 l/s. The geothermal input temperature ranges between 40.6 and 40.9 °C, with the fluctuations of which being in the accuracy range of the temperature sensor. The reinjection temperature is verily load dependent and ranges between 25.5

and 30.5 °C. We consider only steady state operating data for the experimental validation, which are defined as less than $\pm 5\%$ deviation in the measured pumping load over the data collection period of at least 30 min. Fig. A.2 compares the predicted and actual pumping power obtained from the thirteen data sets demonstrating that the model is within $\pm 10\%$ of actual data for almost all operational conditions.

Table A.1

Summarised data of the HBF Stadium well field.

Production well (latitude – 31.95358, longitude 115.77977)	
Casing	8 1/2"/8" (length as indicated in Fig. A.1)
Screened sections	636–684 m and 703–716 m
Efficiency of submersible pump	0.65
Injection well 1 (latitude – 31.95360, longitude 115.77968)	
Casing	5"
Screened sections	560–611 m
Injection well 2 (latitude – 31.95963, longitude 115.78740)	
Casing	8 1/2"/6"/5" (length as indicated in A.1)
Screened sections	572–609 m and 618–633 m
Skin factor wells	1
Overpressure for degassing prevention	3 bar
Potentiometric height water level	–28 m
Lithology of penetrated aquifer	Sandstone, shale, sand, and siltstone dominated High permeability ($k = 0.77$ D)

Fig. A.2 Predicted versus actual pumping power at the well field of HBF Stadium.

A typical set of input data for the pumping model for deep wells, as obtained from the “Cockburn 1” well (latitude – 32.134782, longitude 115.737512) located in the Perth Metropolitan Area, Australia and used for Fig. 5 is shown in Table A.2.

Table A.2

Exemplar input data for geothermal pumping estimation stemming from the “Cockburn 1” well in Western Australia.

Geothermal gradient	2.99	°C/100 m
Flow rate of geothermal fluid	100	kg/s
Salinity of geothermal fluid	15,000	ppm
Potentiometric height	-5	m
Well depth	2162	m
Casing	14"/12" strings of equal length	
Screen height	200	m
Skin factor	1	[–]
Submersible pump depth	250	m
Efficiency of submersible pump [97]	0.72	[–]
Efficiency of injection pump	0.8	[–]
Pressure drop of heat exchanger	0.50	bar
Overpressure for degassing prevention	5	bar
Additional aboveground pressure losses	0.93	bar

Appendix B. Assumptions for the auxiliary power demand of the desalination plant

The auxiliary power demand of the desalination module is estimated based on the media flow rates resulting process simulation under consideration of data adopted from typical market available MED systems as provided in Table B.2 [31].

Table B.2

Considerations for the auxiliary power consumption.

	Head	Pump efficiency	Motor efficiency
Heating medium			
– Basic MED	5 m		
– Booster module	5 m	0.78	0.92
– Pre-heater (each)	5 m		
Brine pump	30 m	0.70	0.92
Distillate pump	40 m	0.50	0.92
Cooling water/feed pump	20 m	0.78	0.92
Ejector pump for NCG removal	30 m	0.78	0.92
Chemical dosing pump		Power rating	
Control panel		0.5 kW	1.5 kW

Appendix C. Desalination plant specifications

In this section all essential parameters such as production rates, specific pumping powers and waste heat performance ratios have been compared among all configurations in each scenario in Table C.1.

Table C.1

Comparison among all configurations in each scenario.

Desalination technology	1500 m			1800 m			2200 m		
	MED	B-MED	PB-MED	MED	B-MED	PB-MED	MED	B-MED	PB-MED
Plant outputs									
Production rate (m ³ /day)	1110	1340	1470	1710	2030	2270	2200	2550	2870
Percentage	n/a	+21%	+32%	n/a	+19%	+33%	n/a	+16%	+30%
Waste heat performance ratio (PR_{WH})	1.62	1.95	2.14	2.09	2.49	2.78	2.41	2.79	3.14
Percentage	n/a	+21%	+32%	n/a	+19%	+33%	n/a	+16%	+30%
Performance ratio (PR)	4.14	4.03	3.91	4.70	4.37	4.23	4.70	4.56	4.37
Percentage	n/a	–3%	–6%	n/a	–7%	–10%	n/a	–3%	–7%
Specific pumping power (kWh/m ³) (desalination plant)	1.58	1.59	1.62	1.40	1.46	1.50	1.40	1.41	1.45
Percentage	n/a	+1%	+3%	n/a	+4%	+7%	n/a	+1%	+4%
Specific pumping power (kWh/m ³) (geothermal and desalination plants)	4.46	4.11	4.03	3.92	3.77	3.71	4.92	4.67	4.58
Percentage	n/a	–8%	–10%	n/a	–4%	–5%	n/a	–5%	–7%

Waste heat performance ratio as in Eq. (C.1) [28], is used instead which encourages the maximal use of the enthalpy of the low grade heat source relative to the heat sink:

$$PR_{WH} = \frac{2326 \cdot D}{\dot{m}_{HS} \cdot (h_{f,HS,in} - h_{f,cond,in})} \quad (C.1)$$

In the above equation 2326 kJ/kg is considered as the enthalpy of distillation.

It should be noted that the conventional performance ratio (Eq. C.2) which holds that heat comes with a premium as it is consumed, cannot capture the essence of such low grade heat driven desalination systems that only attracts a one-off investment cost, other than pumping power [28]. As shown in Table C.1 its trend is incongruent with that of the levelised water costs (Table 4). One can refer to [28] for more details regarding the issue pertaining to performance ratio in low grade heat driven desalination systems.

$$PR = \frac{2326 \cdot D}{\dot{m}_{HS} \cdot (h_{f,HS,in} - h_{f,HS,out})} \quad (C.2)$$

References

- [1] J.C. Bell, Availability of Geothermal Energy for the Demineralization of Saline Water, U.S. Department of the Interior, United States Office of Saline Water, Battelle Memorial Institute, 1959.
- [2] C.M. Wong, Geothermal energy and desalination: partners in progress, *Geothermics*, 2 Part 1 (1970) 892–895.
- [3] A.D.K. Laird, B.W. Tleimat, Desalting geothermal brines, *Desalination* 19 (1976) 309–316.
- [4] W.J. Boegli, S.H. Suemoto, K.M. Trompeter, Geothermal desalting at the East Mesa test site, *Desalination* 22 (1977) 77–90.
- [5] S.H. Suemoto, K.E. Mathias, Preliminary Results of Geothermal Desalting Operations at the East Mesa Test Site, Research for the Development of Geothermal Energy Resources, Imperial Valley, California, 1974 225–235.
- [6] L. Awerbuch, C.T. Draney, Geothermal Energy Recovery Process, U.S. Patent (Ed.), Bechtel International Corporation, 1976.
- [7] A. Ophir, Desalination plant using low grade geothermal heat, *Desalination* 40 (1982) 125–132.
- [8] C. Karytsas, D. Mendlinos, G. Radoglou, The current geothermal exploration and development of the geothermal field of Milos Island in Greece, *GHC Bulletin*. (2004) 17–21.
- [9] M. Yftikas, G. Radoglou, C. Karytsas, D. Mendlinos, A. Vasalakis, N. Andritsos, Geothermal research in Vounalia Area, Milos Island (Greece), for seawater desalination and power production, *Proceedings World Geothermal Congress*, Antalya, Turkey, 2005.
- [10] C. Karytsas, V. Alexandrou, I. Boukis, The Kimolos geothermal desalination project, *International Summer School on Direct Application of Geothermal Energy*, Thessaloniki, Greece 2002, pp. 206–219.
- [11] European Geothermal Energy Council, K4RES-H - Key Issue 5: Innovative Applications Geothermal Utilization for Seawater Desalination, European Renewable Energy Council, 2007.
- [12] P. Ungemach, Energy development problematics in the Mediterranean - the Aeolian and Aegean Islands. The geothermal energy case, *International Workshop on the Possibilities of Geothermal Development of the Aegean Islands Region*, Milos Island, Greece 2002, p. 25.
- [13] J.W. Lund, D.H. Freeston, T.L. Boyd, Direct utilisation of geothermal energy 2010 worldwide review, *Geothermics* 40 (2011) 159–180.
- [14] C. Koroneos, G. Roumbas, Geothermal waters heat integration for the desalination of sea water, *Desalin. Water Treat.* 37 (2012) 69–76.
- [15] A. López-Sánchez, C. Báncora-Alsina, R.M. Prol-Ledesma, G. Hiriart, A new geothermal resource in Los Cabos, Baja California Sur, Mexico, *Proceedings 28th New Zealand Geothermal Workshop*, 2006.
- [16] S.M. Alcocer, G. Hiriart, An applied research program on water desalination with renewable energies, *Am. J. Environ. Sci.* 4 (2008) 190–197.
- [17] J. Gutierrez, M.A. Porta-Gandara, J.L. Fernandez, Distilled water production using geothermally heated seawater, *Desalination* 249 (2009) 41–48.
- [18] H. Gutiérrez, S. Espíndola, Using low enthalpy geothermal resources to desalinate sea water and electricity production on desert areas in Mexico, *GHC Bulletin*. (2010) 6.
- [19] Ministry of Information - Sultanate of Oman, Tap geothermal energy for water desalination, *Business News* - 2, June 2013. (2013).
- [20] A. El Amali, S. Bouguecha, M. Maalej, Experimental study of air gap and direct contact membrane distillation configurations: application to geothermal and seawater desalination, *Desalination* 168 (2004) 357.
- [21] R. Sarbatly, C.-K. Chiamp, Evaluation of geothermal energy in desalination by vacuum membrane distillation, *Applied Energy*, (In Press, Corrected Proof).
- [22] F. Calise, M.D. d'Accadia, A. Macaluso, A. Piacentino, L. Vanoli, Exergetic and exergoeconomic analysis of a novel hybrid solar-geothermal polygeneration system producing energy and water, *Energy Convers. Manag.* 115 (2016) 200–220.
- [23] C. Li, S. Besarati, Y. Goswami, E. Stefanakos, H. Chen, Reverse osmosis desalination driven by low temperature supercritical organic rankine cycle, *Appl. Energy* 102 (2013) 1071–1080.
- [24] S. Loutatidou, H.A. Arafat, Techno-economic analysis of MED and RO desalination powered by low-enthalpy geothermal energy, *Desalination* 365 (2015) 277–292.
- [25] K. Bourouni, R. Martin, L. Tadrist, M.T. Chaibi, Heat transfer and evaporation in geothermal desalination units, *Appl. Energy* 64 (1999) 129–147.
- [26] K. Bourouni, Chaibi, Application of geothermal energy for brackish water desalination in the South of Tunisia, *Proceedings World Geothermal Congress*, Antalya, Turkey, 2005.
- [27] B. Lindal, Industrial and other applications of geothermal energy, *Geothermal Energy - A Review of Research and Development*, Unesco Press, 1973.
- [28] A. Christ, K. Regenauer-Lieb, H.T. Chua, Thermodynamic optimisation of multi effect distillation driven by sensible heat sources, *Desalination* 336 (2014) 160–167.
- [29] X. Wang, A. Christ, K. Regenauer-Lieb, K. Hooman, H.T. Chua, Low grade heat driven multi-effect distillation technology, *Int. J. Heat Mass Transf.* 54 (2011) 5497–5503.
- [30] A. Christ, K. Regenauer-Lieb, H.T. Chua, Application of the Boosted MED process for low-grade heat sources – a pilot plant, *Desalination* 366 (2015) 47–58.
- [31] A. Christ, K. Regenauer-Lieb, H.T. Chua, Boosted multi-effect distillation for sensible low-grade heat sources: a comparison with feed pre-heating multi-effect distillation, *Desalination* 366 (2015) 32–46.
- [32] J.W. Tester, B.J. Anderson, A.S. Batchelor, D.D. Blackwell, R. DiPoppo, E.M. Drake, J. Garnish, B. Livesay, M.C. Moore, K. Nichols, S. Pretty, M.N. Toksoez, R.W. Veatch, *The Future of Geothermal Energy-Impact of Enhanced Geothermal Systems (EGS) on the United States in the 21st Century*, Massachusetts Institute of Technology, Cambridge, 2006 372.
- [33] W.A. Duffield, J.H. Sass, *Geothermal energy-clean power from the earth's heat*, USGS Circular 1249, U.S. Department of the Interior, U.S. Geological Survey, 2003.
- [34] P. Ungemach, *Geothermal reservoir management technology and problem areas*, International Geothermal Days Poland 2004, International Course on Low Enthalpy, Geothermal Resources – Exploitation and Development, Zakopane, Poland, 2004.
- [35] P. Ungemach, M. Antics, *Sustainable geothermal reservoir management practice*, International Geothermal Days 2009, Slovakia, 2009.
- [36] CSIRO Geothermal Energy, *Geothermal Energy and the Perth Basin*, 2013.
- [37] K. Regenauer-Lieb, H.T. Chua, X. Wang, F.G. Horowitz, J.F. Wellmann, Direct heat geothermal applications in the Perth Basin of Western Australia, 34th Workshop on Geothermal Reservoir Engineering, Stanford University, 2009 (pp. SGP-TR-187).
- [38] DesalData.com, *IDA Desalting Plants Inventory*, Media Analytics Ltd. 2011.
- [39] B. Rahimi, A. Christ, K. Regenauer-Lieb, H.T. Chua, A novel process for low grade heat driven desalination, *Desalination* 351 (2014) 202–212.
- [40] G. Polley, C. Haslego, Compact heat exchangers - part 1: designing plate-and-frame heat exchangers, *Chem. Eng. Prog.* 98 (2002) 32–37.
- [41] X. Wang, A. Bierwirth, A. Christ, P. Whittaker, K. Regenauer-Lieb, H.T. Chua, Application of geothermal absorption air-conditioning system: a case study, *Appl. Therm. Eng.* 50 (2013) 71–80.
- [42] C. Teodoriu, C. Cheuffa, A comprehensive review of past and present drilling methods with application to deep geothermal environment Stanford Geothermal Workshop, Stanford, 2011.
- [43] A.J. Mansure, D.A. Blankenship, *Geothermal Well Cost Analyses* 2008, GRC Transactions, 32, 2008.
- [44] Private communication with local Western Australian geothermal drilling companies, 2013.
- [45] F. Horowitz, K. Regenauer-Lieb, J.F. Wellmann, H.T. Chua, X. Wang, T. Poulet, Evidence for hydrothermal convection in the Perth Basin, Australia, in: H. Gurgenci, A.R. Budd (Eds.), *Proceedings of the Sir Mark Oliphant International Frontiers of Science and Technology Australian Geothermal Energy Conference*, Melbourne 2008, pp. 85–87.
- [46] C. Clauer, H. Villinger, Analysis of conductive and convective heat transfer in a sedimentary basin, demonstrated for the Rheingraben, *Geophys. J. Int.* 100 (1990) 393–414.
- [47] Department of Energy, *Revisions to GETEM Model*, 2008.
- [48] D. Entingh, G. Mines, DOE Geothermal Electricity Technology Evaluation Model (GETEM) - Volume III - Detailed Technical Appendices, 2006.
- [49] G. Thiem, *Hydrologische Methoden*, Thesis - (Doctoral) Technische Hochschule Stuttgart, 4 p. I., 56 p., J.m. Gebhardt Verlag Stuttgart, Leipzig, 1906.
- [50] C.W. Fetter, *Applied Hydrogeology*, Fourth Edition ed, Prentice-Hall, New Jersey, 2001.
- [51] M.H. Sharqawy, J.H. Lienhard V, S.M. Zubair, Thermophysical properties of seawater: a review of existing correlations and data, (vol 16, pg 354–380, 2010), *Desalin. Water Treat.* 44 (2010), 361–361.
- [52] D. Entingh, G. Nix, G. Mines, A. Mansure, S. Bauer, S. Petty, B. Livesay, DOE Geothermal Electricity Technology Evaluation Model (GETEM): Volume I – Technical Reference Manual, 2006.
- [53] H.T. El-Dessouky, H.M. Ettouney, F. Mandani, Performance of parallel feed multiple effect evaporation system for seawater desalination, *Appl. Therm. Eng.* 20 (2000) 1679–1706.
- [54] H. El-Dessouky, I. Alatiqi, S. Bingulac, H. Ettouney, Steady-state analysis of the multiple effect evaporation desalination process, *Chem. Eng. Technol.* 21 (1998) 437–451.
- [55] H.T. El-Dessouky, H.M. Ettouney, *Fundamentals of Salt Water Desalination*, Elsevier Science, Burlington, 2002.
- [56] K.H. Mistry, M.A. Antar, J.H. Lienhard V, An improved model for multiple effect distillation, *Desalin. Water Treat.* 51 (2012) 807–821.

- [57] L. Reid, S. Corbel, T. Poulet, L. Ricard, O. Schilling, H.A. Sheldon, J.F. Wellmann, Perth Basin Assessment Program - Project 3: Hydrothermal modelling in the Perth Basin, Western Australia, Western Australian Geothermal Centre of Excellence, Perth, 2012.
- [58] R.D. Hyndman, I.B. Lambert, K.S. Heier, J.C. Jaeger, A.E. Ringwood, Heat flow and surface radioactivity measurements in the Precambrian shield of Western Australia, *Phys. Earth Planet. Inter.* 1 (1968) 129–135.
- [59] T.T. Bestow, The Potential for Geothermal Energy Development in Western Australia, Geological Survey of Western Australia Record 1982/6, Geological Survey of Western Australia, Perth, 1982.
- [60] L.E. Howard, J.H. Sass, Terrestrial heat flow in Australia, *J. Geophys. Res.* 69 (1964) 1617–1626.
- [61] K.A. Ghori, Search for energy from geothermal resources in Western Australia, *Petroleum in Western Australia* 4 (2007).
- [62] K. Regenauer-Lieb, F.G. Horowitz, The Perth Basin geothermal opportunity, *Petroleum in Western Australia* 3 (2007).
- [63] P.N. Chopra, F. Holgate, Geothermal Energy Potential in Selected Areas of Western Australia, for: Government Western Australia, Department of Mines and Petroleum, Weston ACT, Australia, 2008.
- [64] K.A. Ghori, Western Australia's geothermal resources, AAPG Annual Convention & Exhibition, San Antonio, Texas, 2008 2008, p. 15.
- [65] N.E. Timms, S. Corbel, H. Olierook, P.G. Wilkes, C. Delle Piane, H.A. Sheldon, R. Alix, F.G. Horowitz, M.E.J. Wilson, K.A. Evans, C. Griffiths, L. Stützenbecker, S. Israni, P.J. Hamilton, L. Esteban, P. Cope, C. Evans, L. Pimienta, C. Dyt, X. Huang, J. Hopkins, D. Champion, Perth Basin Assessment Program - Project 2: Geomodel, Western Australian Geothermal Centre of Excellence, Perth, 2012.
- [66] L. Ricard, M. Trefry, L. Reid, S. Corbel, L. Esteban, J.-B. Chanu, P.G. Wilkes, G.B. Douglas, A.H. Kaksonen, D. Lester, G. Metcalfe, L. Pimienta, S. Gutbrodt, S. Tressler, G. Bloomfield, C. Evans, K. Regenauer-Lieb, Perth Basin Assessment Program - Project 4: Productivity and Sustainability of Low-Temperature Geothermal Sources, Western Australian Geothermal Centre of Excellence, Perth, 2012.
- [67] Australian Bureau of Statistics, Year Book Australia 2012, 2012.
- [68] Government of Western Australia - Mid West Development Commission, Mid West Development Commission - Climate, 2012.
- [69] Government of Western Australia - Department of Water, City of Geraldton - Greenough - Water conservation plan, Government of Western Australia - Department of Water, Perth, 2010.
- [70] Water and Rivers Commission, Allanooka and Dongara - Denison water reserves water source protection plan: Geraldton and Dongara - Port Denison Town water supplies, Water Resource Protection Series No WRP 47, Water and Rivers Commission, 2002.
- [71] CSIRO, PressurePlot v2.0, 2007.
- [72] B. Hughes, Rig Count, 2013.
- [73] National Centre of Excellence in Desalination in Australia, Australian Desalination Research Roadmap, National Centre of Excellence in Desalination in Australia, Rockingham, Western Australia, 2010.
- [74] B. Schneiders, Four-day pay bonanza, *The Age*, Melbourne, 24.12.2009.
- [75] Australian Bureau of Statistics, Labour Costs Australia 2010–2011, 2012 20.
- [76] B. Mountain, Electricity Prices in Australia: An International Comparison, Energy Users Association of Australia, 2012.
- [77] US Bureau of Labour Statistics, PCU339113339111Z4, 2013.
- [78] Navy Meteorology and Oceanography (METOC) Australia, Coastal Sea Surface Temperatures Australia, 2013.
- [79] Navy Meteorology and Oceanography (METOC) Australia, Coastal Sea Surface Salinities Australia, 2013.
- [80] International Atomic Energy Agency, Desalination Economic Evaluation Program (DEEP 4.0), 2011.
- [81] C. Sommariva, Water Management and Economics, IDA Academy, Singapore, 2012.
- [82] Synergy, Standard Electricity Prices and Charges - South West Interconnected System, Perth, 2012.
- [83] XE, XE Currency Charts (AUD/USD), 2013.
- [84] O. Barron, Desalination options and their possible implementation in Western Australia: potential role for CSIRO land and water, CSIRO: Water for a Healthy Country National Research Flagship, Canberra, 2006.
- [85] Economic Regulation Authority Western Australia, Final report: inquiry on country water and wastewater pricing in Western Australia, Economic Regulation Authority Western Australia, Perth, 2006.
- [86] U.R.S. Australia, Economic and technical assessment of desalination technologies in Australia: with particular reference to national plan priority regions, Prepared for the Department of Agriculture, Fisheries & Forestry - Australia 2002, p. 80.
- [87] M. Hoang, B. Bolto, C. Haskard, O. Barron, S. Gray, G. Leslie, Desalination in Australia, CSIRO, 2009 26.
- [88] O. Barron, K. Zil, Katanning desalination demonstration plant, CSIRO: Water for a Healthy Country National Research Flagship, Canberra, 2006.
- [89] M.K. Withholz, B.K. O'Neill, C.B. Colby, D. Lewis, Estimating the cost of desalination plants using a cost database, *Desalination* 229 (2008) 10–20.
- [90] I. El Saliby, Y. Okour, H.K. Shon, J. Kandasamy, I.S. Kim, Desalination plants in Australia, review and facts, *Desalination* 247 (2009) 1–14.
- [91] T. Pankratz, I.D.A. Desalination Yearbook, Media Analytics Ltd, 2012, Oxford, 2012–2013.
- [92] E. Tzen, Overview of the Desalination Technologies Powered by Renewable Energy, *Desalination Systems Powered by Renewable Energy*, Amman, Jordan, 2006.
- [93] D. Zejli, R. Benchirfa, A. Bennouna, K. Zazi, Economic analysis of wind-powered desalination in the south of Morocco, *Desalination* 165 (2004) 219–230.
- [94] I.C. Karagiannis, P.G. Soldatos, Water desalination cost literature: review and assessment, *Desalination* 223 (2008) 448–456.
- [95] E. Oldmeadow, D. Marinova, Into geothermal solutions: the sustainability case for Challenge Stadium in Perth, Western Australia, *Environmental Progress & Sustainable Energy* 30 (2011) 476–485.
- [96] Challenge Stadium, Geothermal System Operation Manual, 2012.
- [97] Schlumberger, REDA Electric Submersible Pump Technology Catalog, 2011.